

## Hyperfine Splitting and Room-Temperature Ferromagnetism of Ni at Multimegabar Pressure

I. Sergueev,<sup>1,\*</sup> L. Dubrovinsky,<sup>2</sup> M. Ekholm,<sup>3</sup> O. Yu. Vekilova,<sup>4</sup> A. I. Chumakov,<sup>5</sup> M. Zajac,<sup>5</sup> V. Potapkin,<sup>5,2</sup>  
I. Kantor,<sup>5</sup> S. Bornemann,<sup>6</sup> H. Ebert,<sup>6</sup> S. I. Simak,<sup>4</sup> I. A. Abrikosov,<sup>4</sup> and R. Rüffer<sup>5</sup>

<sup>1</sup>Deutsches Elektronen-Synchrotron, D-22607 Hamburg, Germany

<sup>2</sup>Bayerisches Geoinstitut, Universität Bayreuth, D-95440 Bayreuth, Germany

<sup>3</sup>Swedish e-Science Research Centre (SeRC), Department of Physics, Chemistry and Biology (IFM),  
Linköping University, SE-58183 Linköping, Sweden

<sup>4</sup>Department of Physics, Chemistry and Biology (IFM), Linköping University, SE-58183 Linköping, Sweden

<sup>5</sup>European Synchrotron Radiation Facility (ESRF), P.O. Box 220, F-38043 Grenoble, France

<sup>6</sup>Department of Chemistry, Ludwig-Maximilians-Universität München, Butenandtstrasse 11, D-81377 München, Germany

(Received 28 June 2013; published 10 October 2013)

Magnetic and elastic properties of Ni metal have been studied up to 260 GPa by nuclear forward scattering of synchrotron radiation with the 67.4 keV Mössbauer transition of <sup>61</sup>Ni. The observed magnetic hyperfine splitting confirms the ferromagnetic state of Ni up to 260 GPa, the highest pressure where magnetism in any material has been observed so far. *Ab initio* calculations reveal that the pressure evolution of the hyperfine field, which features a maximum in the range of 100 to 225 GPa, is a relativistic effect. The Debye energy obtained from the Lamb-Mössbauer factor increases from 33 meV at ambient pressure to 60 meV at 100 GPa. The change of this energy over volume compression is well described by a Grüneisen parameter of 2.09.

DOI: [10.1103/PhysRevLett.111.157601](https://doi.org/10.1103/PhysRevLett.111.157601)

PACS numbers: 76.80.+y, 31.30.Gs, 62.50.-p, 75.10.-b

Nickel plays a key role in an astonishingly wide range of fields in physics, spanning from microelectronics to the very interior of Earth [1–3]. Like iron and cobalt, it is ferromagnetic, with spontaneous ordering of magnetic moments at ambient conditions. In the simple Stoner model [4,5], the magnetism of such 3*d* transition metals is a result of the competition between itineracy and localization. Because of the higher Coulomb repulsion between the more localized 3*d* electrons, correlations between such electrons become important. By arranging the spins in parallel, the Pauli principle will ensure they stay further apart, which lowers interaction energy, although at the cost of kinetic energy. Depending on the band structure, the balance between these effects may result in fractional spin polarization of the electrons at each lattice site, and hence, a net magnetization.

Application of pressure broadens the band, thus increasing the kinetic energy. At sufficiently high pressure, kinetic energy will dominate, yielding the Stoner nonmagnetic state without any magnetic moments. It is important to distinguish this nonmagnetic state from a paramagnetic state containing disordered local moments without long-range order, which in most magnetic materials is encountered when the temperature exceeds the Curie temperature ( $T_C$ ). A vanishing net magnetization can thus either be due to  $T_C$  being below the experimental temperature or due to quenching of the local moments. In transition metals, the nature of the magnetic ordering has a critical impact on macroscopic properties, such as chemical phase stability [6], even below  $T_C$  [7].

Applying pressure is the most useful way to study the nature of the magnetic state of transition metals, since the balance between Coulomb and kinetic energy can be tuned.

Fe and Co undergo transitions into a nonmagnetic state at 14–25 [8,9] and 100–150 [10–12] GPa at room temperature, respectively. However, in these cases, the collapse of ferromagnetism is associated with structural transitions of the crystal structure. In Ni, on the other hand, the ground state fcc structure is stable at least up to 200 GPa, as confirmed by the x-ray diffraction experiment [13], and it is predicted to be stable up to over 300 GPa [14].

The magnetic moment of Ni has previously been studied by x-ray magnetic circular dichroism [13,15,16] up to 200 GPa and indicates only a slight decrease. Extrapolation of the measured magnetic moment [16] to higher pressures implies a nonmagnetic phase above 250 GPa. Density functional theory (DFT) predicts stability of the local magnetic moments up to at least 300 GPa [17]. At the same time, little attention has been paid so far to the stability of the ferromagnetic *order* of the Ni moments at high pressure. Generally, the Curie temperature decreases with pressure [18], but in Ni, it has been shown to increase up to 8 GPa [19]. At still higher pressure, the behavior of  $T_C$  is largely unknown.

It is thus important to develop new experimental techniques operating at yet higher pressure, in order to investigate the microscopic nature of transition metals, and to complement experiments with theoretical studies for a fundamental understanding of the observed effects. Mössbauer spectroscopy (MS) and its synchrotron radiation counterparts, nuclear forward scattering (NFS) and the synchrotron Mössbauer source, are very efficient methods in high pressure studies of solid state properties, as has been demonstrated for iron containing compounds. MS can also be performed with the isotope <sup>61</sup>Ni, with the nuclear transition energy of 67.4 keV. However, several technical

and fundamental problems restrict the applicability of the method [20], resulting in only a few studies of Ni compounds with MS. The NFS method enables one to overcome some of these problems, and its capability for Ni has recently been demonstrated [21].

In this Letter, we apply NFS to investigate magnetic and elastic properties of Ni at room temperature up to 260 GPa. The magnetic hyperfine splitting at the Ni site was observed up to 260 GPa, which confirms that Ni stays ferromagnetic up to this pressure, the highest pressure where magnetism in any material has been observed so far. Experimental observations are confirmed by theoretical *ab initio* DFT calculations, which reproduce the peculiar pressure dependence of the hyperfine field, and reveal that it is a clear manifestation of relativistic effects. Moreover, by calculating the effective exchange parameter of the classical Heisenberg Hamiltonian [22], we demonstrate that the Curie temperature of Ni depends on pressure quite weakly, in agreement with the experimental observation of a ferromagnetic state in Ni at multimegabar pressure and at room temperature.

Experiments were performed at the nuclear resonance beam line [23] ID18 at the European Synchrotron Radiation Facility. The storage ring was operated in the 16 bunch filling mode with a time window of 176 ns and with an average current of 70 mA. The 67.4 keV incident radiation was monochromatized to  $\sim 30$  meV in two steps by a high heat-load monochromator followed by a medium-resolution monochromator. This monochromator is composed of two pairs of Si(4 4 4) and Si(8 4 4) reflections arranged in a nested configuration. The optical design of the reflections is similar to that one in Ref. [21]. In order to improve the throughput of the monochromators, the radiation was collimated to  $\sim 2$   $\mu$ rad by compound refractive lenses installed upstream of the high heat-load monochromator. The beam after the monochromators was focused by Kirkpatrick-Baez optics to a spot of  $15 \times 15$   $\mu\text{m}^2$  matching the size of the sample in the diamond anvil cell (DAC). The measurements were accomplished by a 16-element array of Si avalanche photodiodes [24] which allowed the separation in time of the electronic and the nuclear resonant scattering.

The metallic Ni foil enriched to 85% in the resonant isotope  $^{61}\text{Ni}$  was used as a sample which was loaded into two DACs. For the pressures below 100 GPa, the sample was loaded together with a small ruby chip (used as a pressure marker) into a Be gasket with a hole of  $\sim 70$   $\mu\text{m}$  diameter. The gasket was mounted into a panoramic-type DAC allowing the measurements perpendicular to and along the DAC axis. For the pressures above 100 GPa, the sample was loaded into a Re gasket with a hole of  $\sim 20$   $\mu\text{m}$  diameter. In this case, the pressure calibration was performed using the Raman shift of diamond. Measurements were performed at room temperature in two geometries, along and perpendicular to the DAC axis. Measurements

along the axis were carried out with both DACs. The sample thickness was less than 15  $\mu\text{m}$ . Measurements perpendicular to the DAC axis were only performed with the sample in the Be gasket, and the sample's thickness was around 70  $\mu\text{m}$ . This geometry with a thick target was used to measure the pressure dependence of the Lamb-Mössbauer factor [21].

The time evolution of the NFS signal, measured at room temperature and at different pressures, is shown in Fig. 1 for the direction along the diamonds and in Fig. 2 for the direction perpendicular to the diamonds. The measurement at ambient pressure was carried out with a Ni foil of 100  $\mu\text{m}$  thickness. The shape of the spectra in Fig. 1 is described by an exponential decay with a 7.6 ns lifetime which is modulated by oscillations, quantum beats, due to the magnetic hyperfine splitting of the nuclear levels. The pressure leads to an increase of the frequency of the quantum beats, while the overall shape of the spectra stays the same. Taking into account the dependence of the spectra on  $Ht$ , where  $H$  is the hyperfine magnetic field and  $t$  is the time, the shrinkage is determined by the increase of the hyperfine magnetic field. The beats observed in the measurements perpendicular to the diamonds (Fig. 2) are “hybrid beats” [25], a combination of quantum and dynamical beats due to the magnetic hyperfine splitting and large effective thickness of the sample. The shift of the beat structure with pressure is mainly due

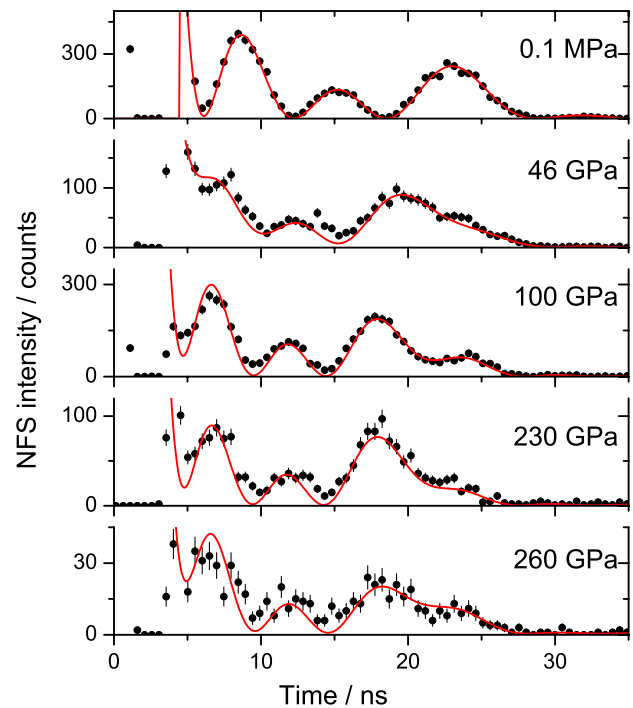


FIG. 1 (color online). Time evolution of the nuclear forward scattering for Ni measured along the DAC axis at room temperature. The solid lines show the fit according to the model described in the text.

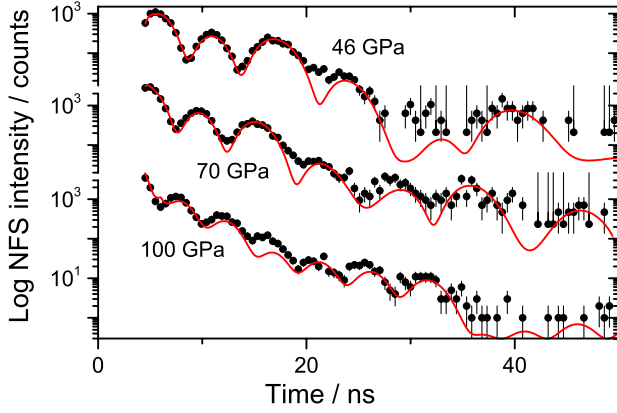


FIG. 2 (color online). Time evolution of the nuclear forward scattering for Ni measured perpendicular to the DAC axis at room temperature. The solid lines show the fit according to the model described in the text.

to the increase of the Lamb-Mössbauer factor which leads to the increase of the effective thickness of the sample.

The fit of the data was performed using a code developed on the basis of the Fourier transformation of the energy spectrum of the nuclear resonance scattering [26] and compared for the not very large effective thickness with the fit by conventional routine [27] for consistency. From the fit, the magnitude of the magnetic hyperfine field and the effective thickness of the samples were obtained. The Lamb-Mössbauer factor was obtained from the effective thickness, assuming the sample thickness of 70(10)  $\mu\text{m}$  for the measurements perpendicular to the diamonds.

Figure 3 shows the measured pressure dependence of the magnetic hyperfine field at room temperature. The magnitude of the field at ambient pressure is 6.90(3) T, which is consistent with previous measurements [28,29]. Upon compression, the magnetic hyperfine field increases, an effect previously observed in nuclear magnetic resonance studies up to 3 GPa [30]. Remarkably, we find the hyperfine field to continue, increasing even up to ultrahigh pressure, reaching 8.85(3) T at 100 GPa. Above 225 GPa, the field seems to decrease, although with a significant field of  $\approx 8.7$  T persisting even in this regime.

In order to confirm this effect and to understand its origin, we carried out theoretical calculations of the hyperfine field within the framework of DFT. We used the local spin density approximation [31] to the exchange-correlation functional, and the experimental equation of state [32]. Figure 3 shows the results as obtained within two levels of approximation to the treatment of relativistic effects: the fully relativistic and the scalar-relativistic approaches. Although the former slightly underestimates the magnitude of the hyperfine field, while the latter overestimates it, the accuracy of the calculations is typical for *ab initio* calculations of the hyperfine field [33]. The most important result is that the fully relativistic treatment, which explicitly includes the spin-orbit coupling,

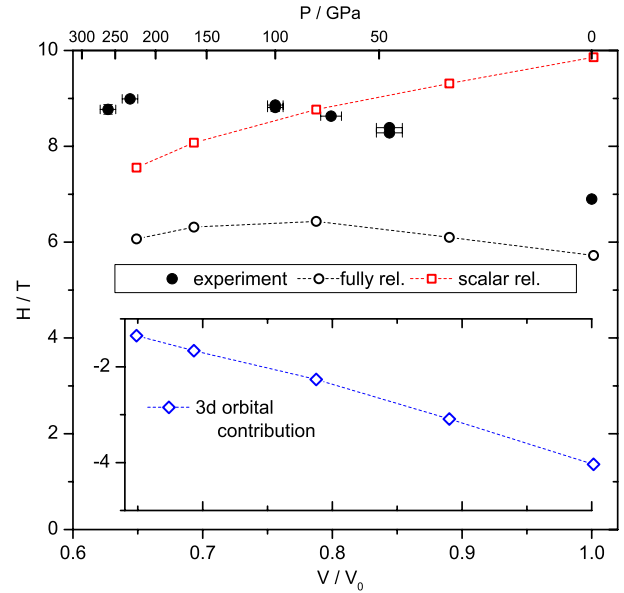


FIG. 3 (color online). Pressure dependence of the hyperfine magnetic field in Ni obtained from the experiment (filled circle) and calculated using scalar-relativistic calculations (open circle) and fully relativistic *ab initio* calculations, explicitly including spin-orbit coupling (square). The inset shows the 3d electron orbital field arising in the fully relativistic calculations.

reproduces all the qualitative features of the measurements: large hyperfine splitting in Ni existing up to highest experimental pressure reached in this work, first increasing up to 100 GPa before dropping slightly at 250 GPa.

It should also be noted that, as is well known [34], the hyperfine field is directed opposite to the total magnetic moment. This can be understood by decomposing the field into core (Ar-atom) and valence ( $3d^84s^2$ ) contributions. Being responsible for the local magnetic moment, the valence spin density is largest where the *d* electron wave function is at its maximum, implying a depletion of majority spin carriers in the vicinity of the nucleus. The core electrons are then polarized locally by exchange interaction with the valence electrons. In fact, the major contribution to the total field is due to the core electrons, which makes up 7.8 T. As pressure is increased, the scalar-relativistic calculations yield a field strength that is decreasing with pressure.

However, by including spin-orbit coupling, the small induced orbital magnetic moment of the 3d electrons ( $0.05\mu_B$ ) will give a crucial contribution, as seen in Fig. 3. The orbital field is directed in parallel with the local magnetic moment and brings the calculations in good agreement with the measurements, reproducing a field strength of 5.7 T at ambient pressure. We attribute the remaining discrepancy in absolute values of the field to the self-interaction error of the local spin density approximation when treating the core polarization contribution [35].

It should be noted that the relation between the magnetic hyperfine field and the magnetic moment is not trivial,

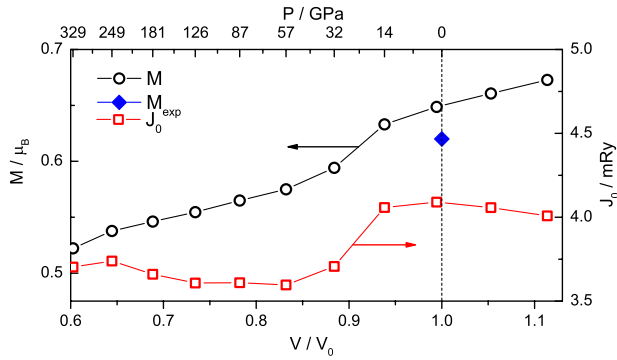


FIG. 4 (color online). Dependence of the calculated magnetic moment  $M$  (circle) and the effective exchange interaction parameter  $J_0$  (square) on the unit cell volume  $V$  normalized with respect to the equilibrium volume  $V_0$  of ferromagnetic fcc Ni. The experimental value of the magnetic moment of Ni at zero pressure [38] is shown for comparison (diamond).

since the magnetic moment is monotonously decreasing with pressure, as shown in Fig. 4. The calculated magnetic moment, shown in Fig. 4, indeed persists up to 300 GPa. However, the magnetic moments calculated for  $T = 0$  K do not directly explain our experiments or x-ray magnetic circular dichroism measurements [13]. Such calculations do not answer the question if the moments, although finite, are still ordered. Since in our case the hyperfine field was measured at room temperature, it unambiguously shows that Ni is in the ordered ferromagnetic state and that, probably, the critical pressure where it becomes paramagnetic at room temperature is at least higher than 300 GPa.

To calculate  $T_C$  in an itinerant magnet such as Ni is a highly nontrivial task [36]. Nevertheless, it is possible to estimate its pressure dependence from the so-called effective exchange parameter  $J_0$  of the classical Heisenberg Hamiltonian [22]. The result  $T_C = (2/3)J_0/k_B$  of classical mean-field theory leads for ambient pressure to a severe underestimated  $T_C$  of Ni [22]. Thus, we focus on the pressure dependence of  $J_0$  itself, keeping in mind that in this way, we should obtain qualitative understanding of the pressure dependence of  $T_C$  (the mean-field approach should provide an estimated lower bound). Figure 4 shows  $J_0$  as a function of pressure. We find that the pressure dependence is very weak, indicating that the Curie temperature in Ni remains above room temperature all the way up to 300 GPa. Our calculations thus support the picture of an ordered ferromagnetic state in Ni at multimegabar pressure.

The pressure dependence of the Lamb-Mössbauer factor  $f_{\text{LM}}$ , measured up to 100 GPa in the direction perpendicular to the DAC axis, is shown in Fig. 5. The Lamb-Mössbauer factor strongly increases with pressure from 0.0041(2) at ambient conditions to 0.18(3) at 100 GPa. Taking into account that the count rate of the nuclear forward scattering is proportional to the square of  $f_{\text{LM}}$ , the pressure increase leads to an improvement of the method efficiency. In particular, the count rate of the

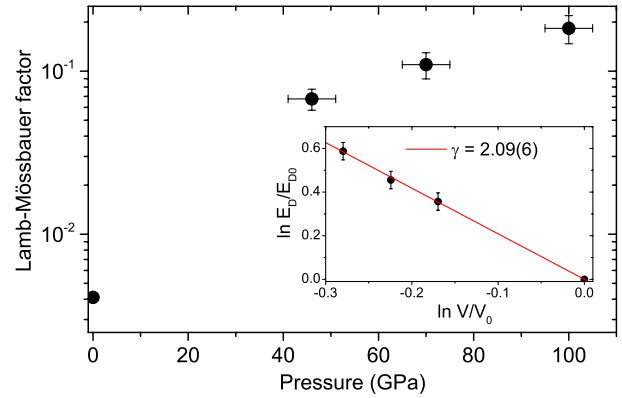


FIG. 5 (color online). Pressure dependence of the Lamb-Mössbauer factor. The inset shows the logarithm of the Debye energy as a function of the logarithm of the volume. The linear fit shown by the line gives the Grüneisen parameter  $\gamma$ .

measurements increased by a factor 10 between 40 and 100 GPa. The characteristic Debye energy  $E_D$  can be obtained from the Lamb-Mössbauer factor using the equation  $\ln f_{\text{LM}} = -6E_R k_B T / E_D^2$ , where  $E_R = 40$  meV is the recoil energy,  $k_B$  is the Boltzmann constant, and  $T = 295$  K is the temperature. The Debye energy increases from 33 meV at ambient pressure to 60 meV at 100 GPa. The absence of a structural phase transition in the studied pressure range allows one to assume that the density of phonon states stretches in energy due to the volume compression. Such stretching is described by the Grüneisen parameter  $\gamma = -d \ln E_D / d \ln V$ . Figure 5 (inset) shows  $\ln E_D / E_{D0}$  as a function of  $\ln V / V_0$ , where  $E_{D0} = 33$  meV is the Debye energy at ambient pressure. It is seen that, indeed, the linear dependence is observed with the Grüneisen parameter of 2.09(6) over the entire pressure range. This value is close to  $\gamma = 1.87$ , observed in Ref. [37] as a softening of Debye energy with temperature. The knowledge of the density of phonon states at ambient pressure and the Grüneisen parameter allows one to calculate the modification of different thermodynamic parameters, like force constant and lattice specific heat. The average sound velocity is proportional to  $E_D$  and increases by  $\sim 2$  at 100 GPa.

In summary, the method of nuclear forward scattering of synchrotron radiation has been applied to study metallic Ni in the pressure range of a few megabars. Measurements of the magnetic hyperfine splitting of the Mössbauer spectrum show that the ferromagnetic order is stable up to at least 260 GPa, the highest pressure that ferromagnetism has been observed so far. Moreover, the pressure dependence of the hyperfine field is seen to be highly nontrivial, increasing up to above 100 GPa before beginning to decrease. This peculiar behavior is explained by our *ab initio* calculations as a relativistic effect, arising from the  $3d$  orbital moment when spin-orbit coupling is included. It is interesting to note that the major contribution to the field strength comes

from core electrons, which may be expected to be less sensitive to changes in external parameters such as pressure; we see a significant pressure dependence, which can be traced directly to the valence electrons.

Our work also demonstrates that the NFS method is well suited to study elastic properties of Ni compounds at the few megabar pressure regime. We find the Debye energy, obtained from the measured Lamb-Mössbauer factor, to show an increase by almost a factor of 2 between ambient pressure and 100 GPa. The dependence of the Debye energy over volume contraction is well described by the Grüneisen parameter 2.09(6). The strong increase of the Lamb-Mössbauer factor with pressure leads to the improvement of the method efficiency at higher pressures.

Generally, the well resolved NFS (time) spectra allow for a precise determination of magnetic phase transitions under compression. Measurements can mainly be performed at temperatures below room temperature, thus allowing for pressure-temperature diagrams for magnetic and elastic properties of materials containing Ni.

The European Synchrotron Radiation Facility is acknowledged for provision of synchrotron radiation beam time and the facility at the beam line ID18. Support from the Swedish Research Council (VR) Projects No. 621-2011-4426 and No. 2011-42-59, LiLiNFM, the Swedish Foundation for Strategic Research (SSF) program SRL10-0026, the Swedish Government Strategic Research Area Grant Swedish e-Science Research Centre (SeRC), and in Materials Science “Advanced Functional Materials” (AFM), as well as SNIC, are gratefully acknowledged. H. E. would like to acknowledge support by the Deutsche Forschungsgemeinschaft (DFG) within Forschergruppe FOR 1346.

---

\*ilya.sergeev@desy.de

- [1] S. S. P. Parkin, M. Hayashi, and L. Thomas, *Science* **320**, 190 (2008).
- [2] R. C. O’Handley, *Modern Magnetic Materials: Principles and Applications* (Wiley, New York, 2000).
- [3] W. F. Bottke, D. Nesvorny, R. E. Grimm, A. Morbidelli, and D. P. O’Brien, *Nature (London)* **439**, 821 (2006).
- [4] E. C. Stoner, *Philos. Mag.* **15**, 1018 (1933).
- [5] E. C. Stoner, *Proc. R. Soc. A* **165**, 372 (1938).
- [6] A. Ruban and I. Abrikosov, *Rep. Prog. Phys.* **71**, 046501 (2008).
- [7] M. Ekholm, H. Zapolsky, A. V. Ruban, I. Vernyhora, D. Ledue, and I. A. Abrikosov, *Phys. Rev. Lett.* **105**, 167208 (2010).
- [8] M. Nicol and G. Jura, *Science* **141**, 1035 (1963).
- [9] D. N. Pipkorn, C. K. Edge, P. Debrunner, G. De Pasquali, H. G. Drickamer, and H. Frauenfelder, *Phys. Rev.* **135**, A1604 (1964).
- [10] C. S. Yoo, H. Cynn, P. Söderlind, and V. Iota, *Phys. Rev. Lett.* **84**, 4132 (2000).
- [11] N. Ishimatsu, N. Kawamura, H. Maruyama, M. Mizumaki, T. Matsuoka, H. Yumoto, H. Ohashi, and M. Suzuki, *Phys. Rev. B* **83**, 180409 (2011).
- [12] R. Torchio, A. Monza, F. Baudelet, S. Pascarelli, O. Mathon, E. Pugh, D. Antonangeli, and J. P. Itié, *Phys. Rev. B* **84**, 060403 (2011).
- [13] R. Torchio, Y. O. Kvashnin, S. Pascarelli, O. Mathon, C. Marini, L. Genovese, P. Bruno, G. Garbarino, A. Dewaele, F. Occelli *et al.*, *Phys. Rev. Lett.* **107**, 237202 (2011).
- [14] T. Jarlborg, *Physica (Amsterdam)* **385C**, 513 (2003).
- [15] N. Ishimatsu, H. Maruyama, N. Kawamura, M. Suzuki, Y. Ohishi, and O. Shimomura, *J. Phys. Soc. Jpn.* **76**, 064703 (2007).
- [16] V. Iota, J.-H. P. Klepeis, C.-S. Yoo, J. Lang, D. Haskel, and G. Srajer, *Appl. Phys. Lett.* **90**, 042505 (2007).
- [17] Y. S. Mohammed, Y. Yan, H. Wang, K. Li, and X. Du, *J. Magn. Magn. Mater.* **322**, 653 (2010).
- [18] P. Mohn, *Magnetism in the Solid State* (Springer, Berlin, 2003).
- [19] J. M. Leger, C. Loriers-Susse, and B. Vodar, *Phys. Rev. B* **6**, 4250 (1972).
- [20] C. A. McCammon, *Can. J. Phys.* **65**, 1294 (1987).
- [21] I. Sergueev, A. I. Chumakov, T. H. Deschaux Beaume-Dang, R. Rüffer, C. Strohm, and U. van Bürck, *Phys. Rev. Lett.* **99**, 097601 (2007).
- [22] A. Liechtenstein, M. Katsnelson, V. Antropov, and V. Gubanov, *J. Magn. Magn. Mater.* **67**, 65 (1987).
- [23] R. Rüffer and A. I. Chumakov, *Hyperfine Interact.* **97–98**, 589 (1996).
- [24] A. Q. R. Baron, S. Kishimoto, J. Morse, and J.-M. Rigal, *J. Synchrotron Radiat.* **13**, 131 (2006).
- [25] Y. V. Shvyd’ko, U. van Bürck, W. Potzel, P. Schindelmann, E. Gerdau, O. Leupold, J. Metge, H. D. Rüter, and G. V. Smirnov, *Phys. Rev. B* **57**, 3552 (1998).
- [26] Y. Kagan, A. M. Afanas’ev, and V. G. Kohn, *J. Phys. C* **12**, 615 (1979).
- [27] Y. V. Shvyd’ko, *Hyperfine Interact.* **125**, 173 (2000).
- [28] M. Shaham, J. Barak, U. El-Hanany, and W. W. Warren, *Phys. Rev. B* **22**, 5400 (1980).
- [29] I. Sergueev, O. Leupold, H.-C. Wille, T. Roth, A. I. Chumakov, and R. Rüffer, *Phys. Rev. B* **78**, 214436 (2008).
- [30] P. C. Riedi, *Phys. Rev. B* **20**, 2203 (1979).
- [31] See Supplemental Material at <http://link.aps.org/supplemental/10.1103/PhysRevLett.111.157601> for computational details.
- [32] A. Dewaele, M. Torrent, P. Loubeyre, and M. Mezouar, *Phys. Rev. B* **78**, 104102 (2008).
- [33] M. Battocletti, H. Ebert, and H. Akai, *Phys. Rev. B* **53**, 9776 (1996).
- [34] J. F. Janak, *Phys. Rev. B* **20**, 2206 (1979).
- [35] H. Ebert, D. Ködderitzsch, and J. Minár, *Rep. Prog. Phys.* **74**, 096501 (2011).
- [36] J. Kübler, *Theory of Itinerant Electron Magnetism* (Oxford Science Publications, Oxford, England, 2000).
- [37] G. K. White, *Proc. Phys. Soc. London* **86**, 159 (1965).
- [38] M. B. Stearns, *Magnetic Properties of Metals—3d, 4d and 5d Elements, Alloys and Compounds*, Landolt-Börnstein: Numerical Data and Functional Relationships in Science and Technology Vol. 19A (Springer Verlag, Berlin, 1986), p. 24.